Energies and Structures of Rotating Argon Clusters: Analytic Descriptions and Numerical Simulations

LAWRENCE L. LOHR

Department of Chemistry, University of Michigan, Ann Arbor, Michigan 48109-1055

Received June 20, 1994; revised manuscript received October 24, 1994; accepted November 28, 1994

ABSTRACT

The dependence of the rotational energy of small argon clusters on the magnitude and direction of their rotational angular momenta is obtained by two different methods, namely, by analytic descriptions parametric in structural variables (centrifugal displacements) and by classical simulations carried out in rotating frames so that rotational angular momenta are conserved. Potential energies are taken as additive Ar_2 pair potentials [R. A. Aziz, J. Chem. Phys. **99**, 4518 (1993)], augmented in some cases by three-body Axilrod–Teller interactions, thus complementing our earlier studies of rare-gas clusters modeled by additive Lennard-Jones oscillator (LJO) pair potentials [L. L. Lohr and C. H. Huben, J. Chem. Phys. **99**, 6369 (1993)]. Quartic and sextic spectroscopic constants are found to be approximately 10% smaller when the Aziz pair potential is used, reflecting its greater stiffness as compared to the LJO potential. The sign of the sextic tensor coefficient for both tetrahedral Ar_4 and octahedral Ar_6 is such that for sufficiently high J the C_{2v} (or D_{2h}) structures with J parallel to a pseudo-C_2 (or true C_2) axis (saddle points on the rotational energy surface at low J) become local energy maxima, the D_{2d} (or D_{4h}) structures with J parallel to an S_4 (or C_4) axis representing the energy minima. The trigonal bipyramidal cluster Ar_5 resembles both Ar_3 and Ar_4 in its rotational characteristics but with reduced manifestations of nonrigidity. As found with an LJO pair potential [D. H. Li and J. Jellinek, Z. Phys. D **12**, 177 (1989)], the icosahedral Ar_{13} cluster displays a very slight preference for D_{3d} structures with J parallel to a C_3 axis, while the D_{5d} structures with J parallel to a C_5 axis are energy maxima and the D_{2h} structures with J parallel to a C_2 axis are saddle points on the rotational energy surface. The scalar quartic spectroscopic coefficient for Ar_{13} is found to be 2.15×10^{-4} times that for the reference diatomic Ar_2. A variety of structural instabilities are described for Ar_{13} clusters with very high rotational energies.

International Journal of Quantum Chemistry, Vol. 57, 707–714 (1996)

CCC 0020-7608 / 96 / 040707-08

Introduction

We recently presented [1a, b] analytic expressions, parametric in centrifugal displacement coordinates, which provide exact classical descriptions of rotational energy dispersions, i.e., the dependence of rotational energy on the magnitude and direction of rotational angular momentum for small nonrigid rare-gas (Rg) clusters modeled by pairwise additive 6-12 Lennard-Jones oscillator (LJO) potential energies. As a complement to our analytic descriptions, our studies also included angular momentum-conserving classical simulations. Specific properties discussed included quartic and higher-order spectroscopic constants for Rg_3, Rg_4, and Rg_6, rotational instabilities for Rg_3, and "cubic" rotational anisotropies for the spherical tops Rg_4 and Rg_6. These studies were extensions of our earlier analytic study [2] of centrifugal distortions in diatomic molecules and our related ab initio studies [3–8] of such distortions in polyatomic molecules.

In the present study, we describe argon clusters by pairwise additive potential energy functions based on the highly accurate 15-parameter diatomic Ar_2 potential reported by Aziz [9]. This function is stiffer than is a LJO potential with the same well depth and equilibrium separation (see Diatomic Ar_2 section), reducing the deformability. For comparative purposes, we studied the same clusters described earlier using the LJO potential. These are the symmetric top triangular Ar_3, the most deformable for a given rotational energy, the spherical top tetrahedral Ar_4, and octahedral Ar_6, whose high symmetry facilitates their description. Additional clusters considered here are the symmetric top trigonal bipyramidal Ar_5, which combines features of Ar_3 and Ar_4, and the spherical top icosahedral Ar_{13}. In some cases, we augmented this assumed cluster potential by the Axilrod–Teller three-body (triple-dipole) interaction [10–13].

Outline of Procedures

ANALYTIC DESCRIPTIONS

The basic outline of our analytic procedures is as before [1a, b], with a generalization of the parametric rotational energy dispersions to an arbitrary pairwise potential. First, consider a diatomic Rg_2 described by a potential energy function $V(r)$ having a well depth ε and an equilibrium separation r_e. Let $v(x)$ be the reduced potential energy V/ε as a function of the reduced separation $x \equiv r/r_e$ and $v'(x)$ be the derivative dv/dx. The J-dependent effective energy v_{eff} may be expressed parametrically in x by the equations

$$v_{eff} = v(x) + (x/2)v'(x) \quad (1a)$$

$$\beta J(J+1) = (x^3/2)v'(x), \quad (1b)$$

where β is the reduced rigid-rotor rotational constant B_e/ε. For the LJO case, we previously [1a] replaced the right-hand side of Eqs. (1a) and (1b) by polynomials in the variable $z \equiv 1/x^2$ (we previously used x to denote the reduced displacement, not the reduced separation as here) and showed that for selected polyatomic clusters described by pairwise additive LJO potentials (i.e., for ones for which a single structural variable suffices for describing the dispersion) the right-hand sides of Eqs. (1a) and (1b) are simply multiplied by integers which we tabulated. These relationships hold in the present, more general case. For example, to describe the dispersion for the tetrahedral cluster Rg_4 with $J \parallel S_4$, simply multiply Eq. (1a) by 2 and Eq. (1b) by 24. Cases requiring two or more structural variables to describe the dispersion typically require three or more parametric equations. For example, consider the cluster Rg_6 with $J \parallel C_3$, producing a molecule with D_{3d} symmetry. The octahedron has six edges at a reduced separation of x in the plane normal to J, six with a smaller reduced separation of y, and three with a reduced separation of z (the *trans* interactions), the last not to be confused with our previous use of z. The dispersion may be described parametrically by the equations

$$v_{eff} = 6v(x) + 6v(y) + 3v(z) + \beta J_3^2/4x^2 \quad (2a)$$

$$\beta J_3^2 = 12x^3v'(x) + 6(x^4/z)v'(z), \quad (2b)$$

in conjunction with the constraints

$$0 = 3y^3v'(y) + (3y^4/2z)v'(z) \quad (2c)$$

$$z^2 = x^2 + y^2. \quad (2d)$$

In the above, β is the reduced rotational constant for the reference diatomic Rg_2, J_3 is the projection of J on the C_3 axis, and v' denotes the derivative of v. Similar sets of equations may be readily obtained for other cases such as Rg_6 with $J \parallel C_4$.

NUMERICAL SIMULATIONS

Our second method [1a, b], used as a complement to the analytic method for the clusters Ar_3, Ar_4, and Ar_6, and as the sole method for the clusters Ar_5 and Ar_{13}, employs a C-language program for carrying out classical mechanical simulations with the imposed constraint of a fixed rotational angular momentum J in the molecular frame. The procedure is summarized as follows:

1. A set of masses $\{m_i\}$ and initial coordinates $\{r_i\}$ are selected, with the center of mass of the cluster taken as the origin.
2. A magnitude and direction for J with respect to the molecular frame is selected, with the direction typically corresponding to a principal axis of the moment of inertia tensor I.
3. The tensor I is calculated from the masses and coordinates; the angular velocity ω is then calculated from $\omega = I^{-1}J$.
4. The force F_i acting on the ith particle is calculated as
$$F_i = -m_i\{\omega \times (\omega \times r_i)\} - \nabla_i V,$$
where the first term represents the J-dependent centrifugal force and the second term arises from the assumed potential energy V.
5. The system is allowed to evolve toward a minimum-energy configuration subject to the constraint of fixed J by assuming a time step Δt, calculating a set of displacements $\{\Delta r_i\}$ from the forces $\{F_i\}$, setting acquired velocities to zero, and repeating the process until the energy has converged.

AZIZ PAIR POTENTIAL

We have assumed that the argon clusters are described by a pairwise additive potential energy function based on the highly accurate Ar_2 potential reported by Aziz [9]. This potential energy function, which represents an improvement over the earlier Aziz–Slaman functions [14, 15], contains damped attractive terms in powers r^{-n}, with $n = 6, 8, 10, 12$, and 14, and fits, within experimental error, the vibrational–rotational levels extracted by Herman et al. from their vacuum UV laser absorption spectrum [16] of Ar_2. The Aziz function contains 15 parameters, including the well depth ε of 99.577 cm^{-1} and the equilibrium separation r_e of 3.7570 Å. In addition, we have included in some of our cluster potential energies the Axilrod–Teller three-body interaction [10–13] which may be written as

$$V_3 = 3Z\left[(3\cos\alpha\cos\beta\cos\gamma + 1)/r_{12}^3 r_{13}^3 r_{23}^3\right], \quad (3)$$

where Z is a parameter calculated [12] to be 176.7 Hartrees a_0^9 for Ar_3 ($Z = 8.4977 \times 10^{-3}$ in reduced units of $\varepsilon\, r_e^9$), α is the angle opposite the edge r_{23}; β, opposite r_{13}; and γ, opposite r_{12}. For an equilateral triangle of edge x, the interaction V_3 is repulsive, namely, $33Z/8x^9$, for a right isosceles triangle it is less repulsive, namely $3Z/8^{1/2}x^9$, while for an equidistant linear array it is attractive, namely, $-3Z/4x^9$. Thus, V_3 for equilateral Ar_3 with $x = 1$ is 0.03505 in units of the well depth ε for Ar_2.

Results and Discussion

DIATOMIC Ar_2

Key properties of Ar_2, such as the harmonic force constant k, the reduced harmonic frequency ω/ε, and the first two vibrational energies ε_0 and ε_1, are all significantly higher with either the Aziz or Aziz–Slaman potentials than with the 6-12 LJO potential having the same well depth and equilibrium separation (the Aziz force constant is about 12% higher than the LJO value, with the vibrational energies also higher). As a consequence of this reduced deformability, the rotational energy dispersion obtained from using the Aziz (or the slightly different Aziz–Slaman) potential differs from that obtained using the LJO by having a maximum in v_{eff} at a somewhat smaller distance (1.1496 vs. 1.1650), a higher v_{eff} at this maximum (1.9992 vs. 1.8), and appreciably smaller (in magnitude) reduced quartic (0.8964 vs. 1) and sextic (−0.7128 vs. −1) coefficients (Table I; the reduced units for d and h are $\beta^2\varepsilon/36$ and $\beta^3\varepsilon/324$, respectively).

TRIANGULAR Ar_3

The important cluster Ar_3 has been the subject of many recent investigations [13, 17–19]. Our analytic description of classical rotation based on use of an arbitrary pairwise additive potential energy is readily obtained for the cases of $J \parallel C_3(D_{3h})$ and $J \parallel C_2(C_{2v})$; for the former case, Eqs. (1a) and (1b) are multiplied by 36 and 3, respectively, while for the latter case, these equations are multiplied by 6

TABLE I
Summary of reduced binding energies and spectroscopic constants for argon clusters[a].

Cluster	BE[b]	BE / n[c]	Case[d]	b[e]	δ[f]	δ(LJO)[g]
Ar_2	1.0	0.5	$J \perp C_\infty$	1.0	0.8964	1.0
Ar_3	3.0	1.0	$J \parallel C_3$	0.5	0.0749	0.0833
			$J \perp C_3$	1.0	0.8987	1.0
Ar_4	6.0	1.5	Scalar	0.5	0.0907	0.1
			Tensor	—	0.0055	0.0062
Ar_5	9.0717	1.8143	$J \parallel C_3$	0.4990	0.0747	—
			$J \perp C_3$	0.2736	0.0168	—
Ar_6	12.5501	2.0917	Scalar	0.2518	0.0101	0.0123
			Tensor	—	0.00085	0.00093
Ar_{13}	43.2227	3.3248	Scalar	0.0644	0.00022	—

[a] Assuming additive Aziz pair potential.
[b] Binding energy in units of well depth $\varepsilon = 99.577$ cm^{-1}.
[c] Binding energy per atom.
[d] Orientation of J (or specification of "scalar" or "tensor" coefficient for spherical tops).
[e] Quadratic coefficient (rotational constant) in units of $B(Ar_2) = 0.05980$ cm^{-1}.
[f] Quartic coefficient in units of $\beta^2\varepsilon/36$ (units for which $\delta = D/\varepsilon = 1$, or $D = 8.312 \times 10^{-8}$ cm^{-1}, for diatomic LJO).
[g] Reduced LJO quartic coefficients from [1a].

and 1, respectively. The case of $J \perp$ to both C_2 and C_3, which we designated as J_y, is described by two structural parameters. This case corresponds to rotation about a pseudo-C_2 axis, meaning that it corresponds to rotation about a true C_2 axis in J-space of the rotational energy surface which has D_{6h} symmetry.

The equations for any of the above three cases may easily be extended to include the Axilrod–Teller interaction, which not only raises the energy slightly but also reduces the second derivative of the energy. Thus, the effect of its inclusion is also to increase slightly the centrifugal displacement for which v_{eff} is a maximum and to decrease slightly the value of this maximum; this increases the magnitudes of both the quartic and sextic coefficients, by approximately 0.5% and 0.1%, respectively, amounts so small that we did not include the three-body interaction in our studies of the dispersions for the larger clusters described below, although we did include it in characterizing the structures of non-rotating Ar_4 and Ar_6.

As previously noted [1a], the orientation of $J \perp C_3$ and $\parallel C_2(J_x)$ for the cluster Rg_3 leads to an obtuse isosceles triangular structure and is slightly favored (lower energy for a given $|J|$) over the acute isosceles triangular structure arising from the case $J \perp C_2(J_y)$. A representative solution of Eqs. (4a–c) for the latter case for Ar_3 with an assumed pairwise additive Aziz potential is that for $\beta J^2 = 1.9487$ (corresponding to $J \approx 56$); the energy $v_{eff} = E_y = 1.8505$, while the structure is characterized by two edges stretched to a reduced distance of 1.0400 and the single edge parallel to J slightly compressed to 0.9886. For this same J, the energy E_x is 1.8250, with one edge stretched to 1.0902 and two edges remaining unchanged ($x = 1$). The corresponding energy E_z is 0.9662, with each of the three edges stretched to 1.009. The fact that E_z is somewhat higher than one-half of E_x or E_y for this planar symmetric top reflects the smaller centrifugal deformability for $J \parallel C_3$ than for $J \perp C_3$. This is also reflected in the very small extension of the edges to 1.009 for the former case as compared to those for the latter. For further comparison, the energy of nonrotating linear Ar_3 is 0.9805, assuming a pairwise additive Aziz potential (0.9790 if the Axilrod–Teller interaction is included).

TETRAHEDRAL Ar_4 AND OCTAHEDRAL Ar_6

Considerable theoretical attention has been devoted, especially by Harter [20, 21], to semirigid spherical top molecules such as CH_4 and SF_6. We included results for the spherical tops Rg_4 and Rg_6 in our studies [1a] of analytic descriptions of LJO rare-gas clusters, with expressions being presented for Rg_4 with $J \parallel S_4(D_{2d})$ and $J \parallel C_3(C_{3v})$ and for Rg_6 with $J \parallel C_4(D_{4h})$, $J \parallel C_3(D_{3d})$, and $J \parallel C_2(D_{2h})$.

A key finding was that the sign of the cubic anisotropy in the rotational energy dispersion is the same for both Rg_4 and Rg_6, and the same as for CH_4, meaning that for a given magnitude of J the six energy minima correspond to $J \parallel S_4$, with the eight equivalent maxima corresponding to $J \parallel C_3$. This is the opposite behavior to that known for SF_6 [20, 21], for which there are six maxima ($J \parallel C_4$) and eight minima ($J \parallel C_3$). An interesting case is that for Ar_4 with J parallel to one of the edges of the tetrahedron, producing a centrifugally distorted molecule of C_{2v} symmetry (the C_2 axis is $\perp$ to J). While this direction for J is not parallel to a symmetry axis of the molecule, it does correspond to a C_2 axis in the centrosymmetric space of the rotational energy surface and is the tetrahedral analog of the $J \parallel C_2(D_{2h})$ case for the octahedral Rg_6 cluster. We refer to this axis as a pseudo-C_2 axis, as it is similar to the rotation of Rg_3 which we described in these terms.

As with Rg_3, the generalized analytic dispersion relationships for the $J \parallel S_4(D_{2d})$ and $J \parallel C_3(C_{3v})$ cases for Rg_4 are simple multiples of the diatomic Rg_2 expressions given in Eqs. (1a) and (1b). Specifically, these equations are multiplied by 24 and 2 in the former case and by 36 and 3 in the latter case. The case of J parallel to a pseudo-C_2 axis for Rg_4 and the three cases of $J \parallel C_4(D_{4h})$, $J \parallel C_3(D_{3d})$, and $J \parallel C_2(D_{2h})$ for Rg_6 are each described by sets of equations, with the set for $J \parallel C_3(D_{3d})$ for Rg_6 being given in Eqs. (2a–d). The sets of equations for the other cases are similar in style to Eqs. (2a–d) and thus not presented here.

Energies for Ar_4 and Ar_6 were obtained independently from our analytic rotational energy dispersions and from our numerical J-conserving simulations. With the latter, the molecules sometimes display abrupt changes in symmetry. For example, using the Aziz pair potential for Ar_4, we find for $J > 100$ that the D_{2d} structures expected for $J \parallel S_4$ acquire D_{2h} symmetry; the molecule has become planar and diamond-shaped. Runs initiated with $J \parallel$ pseudo-C_2 have C_{2v} symmetry for all J and lead to these same planar diamond-shaped D_{2h} structures for $J > 100$ (an increase in symmetry!). Similarly, using the Aziz pair potential for Ar_6, we find for $J > 225$ that the D_{4h} structures expected for $J \parallel C_4$ actually have only C_{2v} symmetry, while the D_{3d} structures with $J \parallel C_3$ and the D_{2h} structures with $J \parallel C_2$ are stable for J up to at least 300.

For Ar_4, we calculated the quartic scalar and tensor spectroscopic constants assuming the pairwise additive Aziz potential. The method is that used previously [1] with the LJO potential and also used in this study for Ar_3, namely, by the evaluation of the limits as βJ^2 approaches zero of centrifugal stabilization energies [1, 2] divided by $(\beta J^2)^2$. In reduced units of $\beta^2\varepsilon/36$, we find (Table I) the scalar coefficient δ_s to be 0.0907 as compared to 1/10 in the LJO case and the tensor coefficient δ_t to be 5.508×10^{-3} as compared to $1/160 = 6.250 \times 10^{-3}$ in the LJO case. For $\beta = 6.005 \times 10^{-4}$ and $\varepsilon = 99.577\ \mathrm{cm}^{-1}$, D_s and D_t are, thus, 9.047×10^{-8} and $5.494 \times 10^{-9}\ \mathrm{cm}^{-1}$, respectively. The reduction in the quartic coefficients by approximately 10% in going from the LJO to the Aziz potential descriptions is quite consistent with the reductions listed (Table I) for Ar_2 and Ar_3. We also list similarly computed values of δ_s and δ_t for octahedral Ar_6, these also showing reductions of approximately 10% in going from the LJO to the Aziz potential descriptions.

TRIGONAL BIPYRAMIDAL Ar_5

A structural type which we did not consider in our LJO studies [1a, b] is the five-atom trigonal bipyramid with D_{3h} symmetry. This is the smallest cluster in which all atom pairs cannot simultaneously be at the diatomic equilibrium separation. We find, using the Aziz pair potential, that the attraction between the two apical atoms causes a slight shortening of the apical to equatorial separation (0.9986) and a slight stretching of the equatorial to equatorial separations (1.0010). The energy of the nonrotating cluster is 0.9283 relative to all pairs being at zero energy with unit separation, or −9.0717 relative to separated atoms. We have considered the three rotational cases analogous to those for Ar_3: These are $J \parallel C_3(z)$, symmetry D_{3h}; $J \parallel C_2(x)$, symmetry C_{2v}; and $J \parallel$ pseudo-C_2 (y), symmetry C_{2v}. In comparing our results to those for Ar_3 and Ar_4, we conclude that the effect of the added atom(s) is to reduce the deformability. The D_{3h} symmetry associated with the $J \parallel C_3(z)$ case appears to be stable up to $J = 130$, above which the symmetry "breaks" to C_{2v}, in the form of a tetrahedron with one atom over an edge parallel to J, the C_2 axis being normal to J. (This edge corresponds to the apical atoms which have closed to a "bonding" distance.) The energy is 4.8244 units above that for $J = 0$; this energy is quite high, being 1.7527 units above that for nonrotating Ar_4 plus Ar and only 0.2473 units below that for nonrotating Ar_3 plus Ar_2. The two cases considered with J in the plane normal to the symmetry axis have very nearly identical energy dispersions; for $J = 100$, the J_y case is higher in energy than is the J_x case by only 1.5×10^{-4} units out of an energy of 1.6424 relative to that for $J = 0$. This same energy obtains for Ar_3 with $J \perp C_3$ with J approximately 53, for which the $J \parallel$ pseudo-$C_2(y)$ case is higher in energy than is the $J \parallel C_2(x)$ case by a very much larger amount, namely, approximately 0.018 units, despite the much smaller J value. Thus, the sextic tensor coefficient representing the deviation of the rotational energy surface from cylindrical symmetry about the J_z axis is negligibly small for Ar_5. The general result, illustrated also in the comparison of Ar_4 and Ar_6 results made above and in the discussion of the Ar_{13} results given below, is that for two clusters of different size (different number of atoms), but with the same rotational energy, the smaller cluster will display the greater effects of nonrigidity, as measured, e.g., by the quartic tensor coefficient for cubic spherical tops or by the sextic tensor coefficient for trigonal symmetric tops and icosahedral spherical tops.

ICOSAHEDRAL Ar_{13}

Icosahedral clusters of rare-gas atoms have been the subject of numerous investigations. Of closest relevance to our investigation is the study by Li and Jellinek [23] of the centrifugally induced distortion and isomerization of Ar_{13} modeled with an LJO pair potential. They have also presented [24, 25] a general formalism for the separation of the energy of rotation in any N-body system, leading to the concept of J-dependent normal vibrational modes. Chartrand et al. studied [26] the effects of the three-body Axilrod–Teller interaction on the structure and dynamics of Ar_{13} and Kr_{13} and found that this interaction lowers the "melting" temperature of the clusters by approximately 10%.

We have used our J-conserving simulation program to study icosahedral Ar_{13} modeled with the Aziz pair potential Specifically, we considered J in steps of 20 from 0 to 400 and steps of 40 from 440 to 1000 for the three cases $J \parallel C_5(D_{5d})$, $J \parallel C_2(D_{2h})$, and $J \parallel C_3(D_{3d})$, cases considered by Li and Jellinek [23] with an LJO pair potential. For $J = 0$, the cluster has an energy of 34.7773 relative to all 78 pair interactions having zero energy, or -43.2227 relative to separated atoms, in units of the reference Ar_2 well depth. This $J = 0$ cluster is characterized by the 30 external edges having a length of 1.0149 and the 12 "radial" distances having a length of 0.9652, both in units of the reference Ar_2 equilibrium separation. As a reference, the similarly computed energy for an Ar_{12} cluster with C_{5v} symmetry has an energy of 28.9384, or -37.0616 relative to separated atoms. Thus, the energy to remove one atom from Ar_{12} is 6.1611, which is approximately the energy to break six Ar–Ar "bonds." Because of its icosahedral (I_h) symmetry, the leading tensor (nonspherical) term in the rotational Hamiltonian for Ar_{13} is sixth power in J; as a consequence, the icosahedral anisotropy in the rotational energy is quite small. For example, with $J = 400$, the energies E_5, E_2, and E_3, corresponding to the three cases $J \parallel C_5(D_{5d})$, $J \parallel C_2(D_{2h})$, and $J \parallel C_3(D_{3d})$, respectively, have energies of 6.4060, 6.4056, and 6.4055 above that for $J = 0$. (Note that these energies are slightly above the dissociation limit to form Ar_{12} plus Ar.) Thus, rotation with $J \parallel C_3$ is preferred, but only by 0.0005, or about 0.008% of its rotational energy, over rotation with $J \parallel C_5$. The case $J \parallel C_2(D_{2h})$ corresponds to the saddle points on the rotational energy surface and is seen to be only very slightly higher in energy than is the D_{3d} minima. Thus, the relative energies for these three cases are the same as those found by Li and Jellinek with their LJO model. They also found that new structures are produced in the C_2 and C_3 cases for $L = 550$ (in units of $1.57\hbar$), with fragmentation occurring at $L = 650$ for C_2 and 700 for C_3. Our results are similar, differing slightly in detail. We find the $D_{5d}(J \parallel C_5)$ structure to be "stable" up to $J = 1000$ (in units of $\hbar$), with an energy of 37.9532 above that for $J = 0$, while the $D_{2h}(J \parallel C_2)$ and $D_{3d}(J \parallel C_3)$ structures are nearly identical in energy up to $J = 840$; the latter is very slightly favored up to this value, although the former (D_{2h}) structure has a lower energy for still higher J. Near $J = 900$, the D_{2h} symmetry structure for $J \parallel C_2$ passes through a tetracapped cube structure having D_{4h} symmetry (a fragment of a body-centered structure) to form a structure having only C_{2v} symmetry [Fig. 1 (a) and (b)]. This change results from the triangles having J passing through the midpoint of their shared edges opening up to form a square. In this same range, the D_{3d} structure associated with $J \parallel C_3$ also undergoes a symmetry breaking, namely, to a structure having the chiral symmetry C_3 [Fig. 1 (c) and (d)].

What does one make of these instabilities? First, for Ar_{13}, they occur at quite high energies, typically 30 units (of the reference diatomic dissocia-

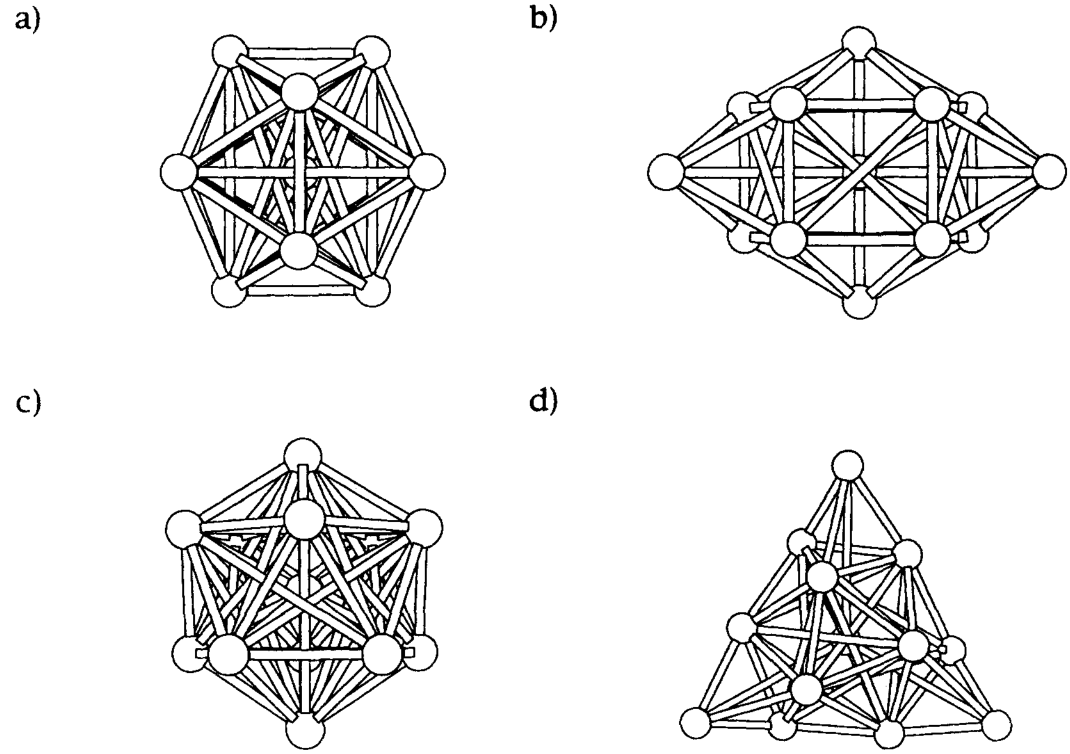

FIGURE 1. Structure of icosahedral (I_h) Ar_{13} ($J = 0$), viewed along C_2 axis; (b) same with $J \parallel C_2$ ($J \cong 900$), the D_{2h} structure converts to C_{2v} symmetry; (c) structure of icosahedral (I_h) Ar_{13} ($J = 0$), viewed along C_3 axis; (d) same with $J \parallel C_3$ ($J \cong 900$), the D_{3d} structure converts to the chiral symmetry C_3.

tion energy), far more than that needed to detach a single atom, so that they are unlikely to be of experimental significance. Nonetheless, they illustrate the richness of structures accessible for clusters with high rotational angular momenta. Second, some of them conserve the symmetry of the low-J centrifugally distorted structures; others do not. An example of the former is the abrupt collapse of the slightly compressed D_{4h} structure of Ar_6 with $J \parallel C_4$ to a D_{4h} structure with the apical atoms "touching," while an example of the latter is the reduction of symmetry to C_{2v} at still higher J. The absence of symmetry breaking is not a valid criterion for a stable equilibrium as it may simply indicate that the molecule is stuck in an unstable equilibrium. Third, the examples described above, and those described by Li and Jellinek [23], do serve to illustrate the rich variety of structures, nearly degenerate in energy, which obtain for rare-gas clusters with high rotational energy.

We have extracted (Table I) from our energies a reduced scalar quartic coefficient δ_s (as mentioned above, there is no tensor quartic coefficient) for Ar_{13} of 2.15×10^{-4} in units of $\beta^2/36\varepsilon$, the units for which δ equals 1.0 for the reference diatomic Ar_2. This δ_s is indeed quite small, although since the rigid-rotor constant for Ar_{13} is 0.0644 times that for Ar_2, a given rotational energy for Ar_{13} corresponds to a much larger J value than the same energy does for Ar_2, so that for a given energy, J^4 (Ar_{13}) is about 220 times J^4 (Ar_2), thus making the effect of the quartic term for Ar_{13} approximately 10^{-2} rather than 10^{-4} times that for Ar_2.

We also considered the cube-octahedral Ar_{13} cluster with O_h symmetry. For $J = 0$, the energy is 38.4554, which is 3.6781 units above that of the I_h structure, and the nearest-neighbor separations are 0.9924. The energies rise more slowly with J than do those starting from the I_h structure, and then drop, with the structures changing at relatively low rotational excitations. Specifically, near $J = 120$, both the $J \parallel C_4(D_{4h})$ and $J \parallel C_2(D_{2h})$ cases become identical to the $J \parallel C_2(D_{2h})$ case originating from the I_h structure, while near $J = 200$, the $J \parallel C_3(D_{3d})$ case becomes identical to that with $J \parallel C_3(D_{3d})$ originating from the I_h structure.

Summary

In this study, we extended both the analytic description of the rotational energy dispersions of rare-gas clusters and the angular momentum-conserving simulation procedure to include the highly accurate Ar—Ar pair potential of Aziz [9] augmented in some cases by the three-body Axilrod–Teller interaction. In addition to the three-, four-, and six-atom systems that we considered in our earlier study [1] based on Lennard-Jones pair potentials, we presented here results obtained by the simulation method for the icosahedral cluster Ar_{13}. Results for the clusters Ar_n, with n ranging from 7 to 147, will be presented elsewhere [27]. The central product of any of these studies is a description of the structure and energy of a rare-gas cluster having a given magnitude and direction of its rotational angular momentum, while special features of the rotational energy dispersions are highlighted by the extraction of quartic and sextic spectroscopic constants. Each J-dependent structure and energy thus represents a reference point about which the molecule having that J vibrates. Consequently, the results presented here serve as approximate descriptions of the ground vibrational state of each cluster. This is illustrated by Ar_2, for which the observed ratio of B_o to be B_e is [16] 0.05776 cm^{-1}/0.05965 cm^{-1} = 0.9683, while that of D_o to D_e is 1.22×10^{-6} cm^{-1}/0.896×10^{-6} cm^{-1} = 1.36; as v increase, the ratio B_v/B_o falls while D_v/D_o rises. We further note that the zero-point energy [16] for Ar_2 is 14.8 cm^{-1}, or 0.149 in units of its well depth, while that [19] for Ar_3 is 43.9 cm^{-1}, which is nearly the same fraction (0.147) of its well depth, suggesting a rough constancy in the relative magnitude of the zero-point energy. To the extent that rotation about a principal axis may be considered separable from other degrees of freedom, the accompanying displacement along a centrifugal distortion pathway may be treated as a single degree of freedom describable semiclassically in the same manner [28] as the stretching of a rotating diatomic, i.e., evaluation of the first-order vibrational action integral as a function of energy and angular momentum will provide the information needed to obtain the rotational energy dispersion for a specified vibrational action (vibrational state).

ACKNOWLEDGMENT

The author wishes to thank Mr. Carl H. Huben for his assistance with the angular momentum-conserving simulation program.

References

1. (a) L. L. Lohr and C. H. Huben, J. Chem. Phys. **99**, 6369 (1993). (b) L. L. Lohr and C. H. Huben, *Mathematical Computation with MapleV: Ideas and Applications. Proceedings of the Maple Summer Workshop and Symposium, 1993*, T. Lee, Ed. (Birkhäuser, Boston, 1993), pp. 137–143.
2. L. L. Lohr, J. Mol. Spectrosc. **155**, 205 (1992).
3. L. L. Lohr and J. -M. Popa, J. Chem. Phys. **84**, 4196 (1986).
4. L. L. Lohr and A. J. Helman, J. Comput. Chem. **8**, 307 (1987).
5. L. L. Lohr, Int. J. Quantum Chem. Symp. **21**, 407 (1987).
6. A. Taleb-Bendiab and L. L. Lohr, J. Mol. Spectrosc. **132**, 413 (1988).
7. L. L. Lohr, J. Mol. Struct. (Theochem) **199**, 265 (1989).
8. L. L. Lohr, J. Mol. Spectrosc. **162**, 300 (1993).
9. R. A. Aziz, J. Chem. Phys. **99**, 4518 (1993).
10. B. M. Axilrod and E. Teller, J. Chem. Phys. **11**, 299 (1943).
11. R. J. Bell and I. J. Zucker, *Rare Gas Solids*, M. L. Klein and J. A. Venables, Eds., (Academic Press, London, 1976), Vol. 1, pp. 122–175.
12. A. Kumer and W. J. Meath, Mol. Phys. **54**, 823 (1985).
13. T. R. Horn, R. B. Gerber, J. J. Valentini, and M. A. Ratner, J. Chem. Phys. **94**, 6728 (1991).
14. R. A. Aziz and M. J. Slaman, Mol. Phys. **58**, 679 (1986).
15. R. A. Aziz and M. J. Slaman, J. Chem. Phys. **92**, 1030 (1990).
16. P. R. Herman, P. E. LaRocque, and B. P. Stoicheff, J. Chem. Phys. **89**, 4535 (1988).
17. C. Amitrano and R. S. Berry, Phys. Rev. Lett. **68**, 729 (1992).
18. R. J. Hinde, R. S. Berry, and D. J. Wales, J. Chem. Phys. **96**, 1376 (1992).
19. A. R. Cooper, S. Jain, and J. M. Huston, J. Chem. Phys. **98**, 2160 (1993).
20. W. G. Harter, Comput. Phys. Rep. **8**, 319 (1988).
21. W. G. Harter, *Principles of Symmetry, Dynamics, and Spectroscopy* (Wiley, New York, 1993).
22. (a) K. T. Hecht, J. Mol. Spectrosc. **5**, 355 (1960); (b) *Ibid.* **5**, 390 (1960).
23. D. H. Li and J. Jellinek, Z. Phys. D **12**, 177 (1989).
24. J. Jellinek and D. H. Li, Phys. Rev. Lett. **62**, 241 (1989).
25. J. Jellinek and D. H. Li, Chem. Phys. Lett. **169**, 380 (1990).
26. D. J. Chartrand, R. J. LeRoy, A. Kumar, and W. J. Meath, J. Chem. Phys. **98**, 5668 (1993).
27. L. L. Lohr, Mol. Phys., in press.
28. R. J. LeRoy, *Semiclassical Methods in Molecular Scattering and Spectroscopy*, NATO ASI Series C, Vol. 53, M. S. Child, Ed. (D. Reidel, Dordrect, Boston, London, 1980), pp. 109–126.